PAPER

Check for updates

In vivo evaluation of compliance mismatch on intimal hyperplasia formation in small diameter vascular grafts†

Yuan Yao, [iD] ‡[a] Grace Pohan,‡[a] Marie F. A. Cutiongco, [iD] §[b,c] YeJin Jeong, [iD] [a] Joshua Kunihiro, [iD] [a] Aung Moe Zaw,[a] Dency David,[a] Hanyue Shangguan,[d,e,f] Alfred C. H. Yu [iD] [d,e,f] and Evelyn K. F. Yim [iD] *[a,b,e,f]

Small diameter synthetic vascular grafts have high failure rate due to the thrombosis and intimal hyperplasia formation. Compliance mismatch between the synthetic graft and native artery has been speculated to be one of the main causes of intimal hyperplasia. However, changing the compliance of synthetic materials without altering material chemistry remains a challenge. Here, we used poly(vinyl alcohol) (PVA) hydrogel as a graft material due to its biocompatibility and tunable mechanical properties to investigate the role of graft compliance in the development of intimal hyperplasia and *in vivo* patency. Two groups of PVA small diameter grafts with low compliance and high compliance were fabricated by dip casting method and implanted in a rabbit carotid artery end-to-side anastomosis model for 4 weeks. We demonstrated that the grafts with compliance that more closely matched with rabbit carotid artery had lower anastomotic intimal hyperplasia formation and higher graft patency compared to low compliance grafts. Overall, this study suggested that reducing the compliance mismatch between the native artery and vascular grafts is beneficial for reducing intimal hyperplasia formation.

1. Introduction

Cardiovascular disease remains the leading cause of death around the globe, representing 32% of deaths worldwide.[1] Vascular reconstruction surgeries are common surgical interventions to restore blood perfusion. Autologous grafts, such as internal thoracic arteries and saphenous veins from patients, are common vascular graft choices; however, autologous grafts have limited availability.[2] Vascular grafts made of synthetic materials, such as expanded polytetrafluoroethylene (ePTFE) or

[a]Department of Chemical Engineering, University of Waterloo, 200 University Avenue West, Waterloo, ON, Canada N2L 3G1. E-mail: eyim@uwaterloo.ca

[b]Mechanobiology Institute, National University of Singapore, 9 Engineering Drive 1, Singapore 117575

[c]Division of Cell Matrix Biology and Regenerative Medicine, The University of Manchester, Oxford Road, Manchester, UK M13 9PL

[d]Schlegel Research Institute for Aging, University of Waterloo, 200 University Avenue West, Waterloo, ON, Canada N2L 3G1

[e]Waterloo Institute for Nanotechnology, University of Waterloo, 200 University Avenue West, Waterloo, ON, Canada N2L 3G1

[f]Center for Biotechnology and Bioengineering, University of Waterloo, 200 University Avenue West, Waterloo, ON, Canada N2L 3G1

†Electronic supplementary information (ESI) available. See DOI: https://doi.org/10.1039/d3bm00167a

‡Authors contribute equally.

§Current address: School of Chemistry of Chemical Engineering and Biotechnology, Nanyang Technology University, Singapore.

polyethylene terephthalate (PET), are currently used as alternative to autologous grafts, and have shown satisfactory patency when replacing large diameter (>6 mm) vessels.[3,4] However, currently available small diameter synthetic vascular grafts have low patency rate due to thrombosis and intimal hyperplasia formation.[5] The absence of endothelial cell coverage on the luminal surfaces of synthetic grafts and the compliance mismatch between the synthetic vascular graft and native artery have been proposed as the main causes of graft failure.[6,7]

Compliance mismatch has long been hypothesized to promote intimal hyperplasia formation,[8,9] which is detrimental to the patency of vascular grafts. Intimal hyperplasia is frequently observed at the anastomotic regions, and biophysical and biomechanical factors, such as anastomotic geometry and mechanical properties of vascular grafts, are important contributors.[10–12] Computational fluid dynamics studies have demonstrated that implantation of non-compliant vascular grafts disturbs blood flow patterns, creating flow separation, recirculation and stagnation zones near the distal anastomoses.[13] Compliance mismatch has also been shown to decrease wall shear stress, create oscillating wall shear stress, and increase suture line stresses.[14,15] All these effects could cause endothelial injury and activation, smooth muscle cell migration and proliferation, and ultimately intimal hyperplasia formation.[16,17] Although many simulation studies have demonstrated the potential role of compliance mismatch in

the development of intimal hyperplasia, most simulation studies were developed based on simplified assumptions and do not accurately represent *in vivo* flow conditions. Additionally, contradictory *in vivo* results were reported. Some studies found that compliance mismatch significantly promoted intimal hyperplasia,[18–20] while others suggested that compliance alone had minimal effect.[21] *In vivo* studies demonstrating compliance matching grafts could reduce intimal hyperplasia were mainly comparing synthetic grafts with autologous grafts. Few studies directly relate compliance-mismatch and the resulting changes in the development of intimal hyperplasia *in vivo* because of confounding factors of graft properties.[22] Thus, clinically relevant *in vivo* studies using synthetic vascular grafts with tunable compliance without affecting material chemistry are needed to elucidate the effect of compliance mismatch on intimal hyperplasia formation and graft patency.

Poly(vinyl alcohol) (PVA) is a non-toxic polymer and has been widely used in various biomedical applications.[23] PVA-based hydrogels have also shown potential in tissue engineering.[24] Our previous studies demonstrated that the PVA hydrogels crosslinked by sodium trimetaphosphate (STMP) have good biocompatibility and low platelet adhesion and low thrombin generation,[25–27] suggesting the STMP-crosslinked PVA hydrogel is a promising vascular graft material. Additionally, we developed a dip cast method to fabricate small diameter PVA vascular grafts, allowing us to manipulate the mechanical properties of the PVA vascular grafts by changing the number of dip coating layers.[27] Our previous study showed that by reducing the number of dip coating layers, we were able to reduce the thickness and increase the compliance of PVA vascular grafts without the need of additional chemical modification.[28]

In this study, we use PVA small diameter vascular grafts fabricated with different thicknesses to systematically study the effect of compliance mismatch on the intimal hyperplasia formation in an *in vivo* rabbit model. We hypothesize that compliance mismatch has a direct effect on intimal hyperplasia formation, and the decrease in compliance mismatch will reduce intimal hyperplasia formation and improve graft patency. Small diameter PVA vascular grafts were fabricated by dip casting method. We implanted PVA small diameter grafts with different compliance in a rabbit carotid artery end-to-side model and examined the graft performance and intimal hyperplasia formation. Our study demonstrated decreasing compliance mismatch between graft and native artery has a beneficial effect on graft patency.

2. Materials and methods

2.1. Fabrication of PVA tubular grafts

PVA grafts were fabricated by dip casting method as previously reported.[27] Briefly, 10% (w/v) PVA (Sigma-Aldrich, 85–124 kDa, 87–89% hydrolyzed) solution was prepared by dissolving PVA in deionized (DI) water at 121 °C for 20 min 30 mL 10% PVA solution was mixed thoroughly with 2.5 mL 15% (w/v) STMP (Sigma-Aldrich) solution, followed by the addition of 1 mL 30% (w/v) sodium hydroxide (NaOH, Sigma-Aldrich) solution.

The mixture was stirred to ensure homogeneity and subsequently centrifuged to remove bubbles. After centrifuge, the PVA crosslinking solution was used directly for fabrication.

To fabricate tubular grafts, flexible metal cylinder rods were used as dipping molds. The molds were treated with air plasma for 1 minute. The freshly plasma-treated molds were immersed immediately in crosslinking PVA solution and dip-coated with PVA crosslinking solution repeatedly, as shown in Fig. 1A. The grafts with different compliance were fabricated by adjusting the number of dips. Upon completion of the last dip, the PVA-coated molds were moved in a cabinet with controlled temperature (20 °C) and humidity (60%–70%). To fabricate curved grafts, after overnight crosslinking in the cabinet, the PVA-coated molds were bent on a cylinder rod and continued to crosslink in cabinet for 3 days.

2.2. Wall thickness measurement

To determine the wall thickness of PVA tubular grafts, 1 mm length cross-sectional segments were made by cutting the graft with a blade at different regions along the graft. The cross-sections of the PVA ring were imaged with a camera, and the thicknesses were measured in ImageJ. For each individual graft, the wall thickness values of different regions were averaged to get the wall thickness results for the graft.

2.3. Burst pressure measurement

To determine burst pressure, the PVA graft was clamped at one end and the other end was connected to a nitrogen gas cylinder.[28] A pressure regulator was used to control the gas supply to gradually increase the pressure. The pressure at which the graft burst was recorded as burst pressure.

2.4. Compliance measurement

Compliance of PVA tubular grafts was determined by measuring the outer diameter change at internal pressure of 80 mmHg and 120 mmHg.[28] One end of the PVA graft was
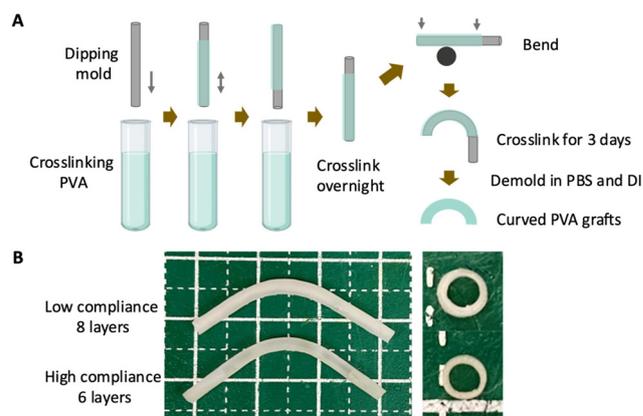

Fig. 1 Fabrication of PVA small diameter vascular grafts with low compliance (LC) and high compliance (HC). (A) Schematic diagram of PVA small diameter vascular graft fabrication procedure. (B) Representative pictures of low compliance and high compliance PVA grafts.

clamped and fixed on a cutting board. The other end of the graft was connected to a saline bag through an intravenous administration tubing. The 80 mmHg and 120 mmHg internal pressure was achieved by changing the height of the saline bag. The graft was imaged with a camera, and the outer diameter of the graft when being exposed to internal pressure of 80 mmHg (D_{80}) and 120 mmHg (D_{120}) was measured in ImageJ. The compliance was calculated using the equation: Compliance (%/40 mmHg) = $(D_{120} - D_{80})/D_{80} \times 100\%$. Each graft was measured at 9 regions along the graft and the average compliance value was recorded as the compliance of the graft.

2.5. Implantation of PVA vascular grafts in rabbit right common carotid artery end-to-side anastomosis model

PVA grafts with low compliance and high compliance were sterilized with gamma irradiation,[29] and subsequently implanted in rabbit right common carotid artery with end-to-side anastomosis technique, as previously reported.[30] Studies were done in accordance with approved protocol (AUPP 18-10 and AUPP 16-09) by the Animal Care Committee according to the Canadian Council on Animal Care's Guidelines. Briefly, 9 male New Zealand White rabbits (Charles River laboratories, body weight of 3.5–4.0 kg) were used in this study. Animals were randomly separated into 2 groups: low compliance group (n = 5) and high compliance group (n = 4). During the surgery, the animals were anaesthetized with 2–3% gas isoflurane through endotracheal intubation. The right common carotid artery of the animal was exposed. Anticoagulant (heparin, 200 IU kg^{-1}) was given intravenously prior to arterial clamping. Five low compliance PVA graft and four high compliance PVA grafts with inner diameter of 1.7 mm, length of 2 cm, and curvature of 1.4 cm radius in the middle were implanted on the rabbit right common carotid arteries with interrupted suturing. Ultrasound imaging were done at 10–14 days (midpoint) after surgery and 27–30 days (endpoint) after surgery to detect blood flow and graft patency using SonixTouch (Analogic Ultrasound, Peabody) or Siemens Acuson (X300 ultrasound system). All scans were done with a 10.0 MHz linear array transducer. Imaging focal depth was positioned at the center of the graft lumen. Image persistence settings were enabled to yield images with reduced speckle appearance. Image-guided Doppler spectrogram measurements (10 MHz frequency, 1–10 kHz pulse repetition frequency) were also performed to assess the graft's flow velocity profile over time. The Doppler range gate was positioned at the center of the graft lumen, and angle correction was 60–70°.

2.6. Tissue processing and histological analysis

The standard practice to investigate stenosis and intimal hyperplasia requires pre-mortal pressurized perfusion. However, due to animal ethical protocol limitation, pre-mortal perfusion could not be performed. To harvest the graft at endpoint, the animals were administrated with heparin (500 IU) and euthanized with sodium pentobarbital (100 mg kg^{-1}). The PVA grafts and the connected native arteries were explanted and fixed in 4% paraformaldehyde (PFA) for 72 h. After fixation, the samples were dehydrated and embedded in paraffin.

The paraffin-embedded tissue blocks were then sectioned with a microtome at the proximal and distal anastomoses.

Hematoxylin and eosin (H&E) staining, Masson's trichrome staining, and immunohistochemistry staining were done on the cross-sectional tissue slides from the anastomoses. The stained slides were imaged with a microscope and analyzed in ImageJ software. H&E-stained slides were used to analyze the intimal hyperplasia percentage by dividing the area of intimal hyperplasia to the total luminal area of anastomoses. Masson's trichrome staining was done with a Trichrome staining kit (Abcam) according to the supplier's protocol. The images of the Masson's trichrome-stained slides were processed with a Color Deconvolution software in ImageJ. The area of collagen and muscle fibers were measured in ImageJ and the percentage was calculated by dividing the area of collagen or muscle fibers to the total luminal area of anastomoses and the area of the intimal hyperplasia. Immunohistochemistry (IHC) staining of α-smooth muscle actin (α-SMA), smooth muscle myosin heavy chain (MHC), and smooth muscle protein 22α (SM22α) was done to visualize smooth muscle cells and characterize smooth muscle cell phenotype. The IHC staining was performed with Abcam mouse HRP/DAB (ABC) detection IHC kit, with primary antibodies of mouse anti-α-SMA, mouse anti-smooth muscle MHC I, and goat anti-TAGLN/Transgelin antibody from Abcam, and biotinylated goat anti-mouse or donkey anti-goat secondary antibodies. The samples were counter-stained with hematoxylin from Abcam. The quantification of IHC staining was done in Fiji with a color deconvolution function. The percentage of positive area was calculated by dividing the area of positive region to the area of intimal hyperplasia.

2.7. Statistical analysis

Statistical analysis was performed using GraphPad Prism 8. The data were presented as mean ± Standard Deviation (SD). The number of biological replicas was indicated in the legend of each figure. Statistical analysis was done with t-test and two-way ANOVA with Sidak's *post hoc* test. Statistical significance was set to be $p < 0.05$.

2.8. Ethical statement

Rabbit end-to-side studies were approved (#AUPP 16-09 and #AUPP 18-10) by the Animal Care Committee according to the Canadian Council on Animal Care's Guidelines, the requirements of Province of Ontario's Animals for Research Act, and the University of Waterloo's Guidelines for the Use of Animals in Research and Teaching. Rabbit end-to-end studies were done in accordance with approved guidelines of the Institutional Animal Care and Use Committee of the National University of Singapore.

3. Results

3.1. Fabrication of grafts with low compliance (LC) and high compliance (HC)

PVA grafts with low compliance (LC) and high compliance (HC) were fabricated as shown in Fig. 1A. LC grafts were fabri-

cated with 8 layers of dip casting while HC grafts were fabricated with 6 layers of dip casting. Photos of LC and HC grafts showed that LC grafts were thicker compared to HC grafts (Fig. 1B). Both the LC and HC grafts were curved during the fabrication to avoid kinking after implantation. The measurement of wall thickness showed that LC grafts had an average wall thickness of 0.409 ± 0.047 mm, which is significantly higher than HC grafts, which has a wall thickness of 0.269 ± 0.034 mm ($P = 0.0133$, $n = 3$) (Fig. 2A). The different wall thickness also yielded distinct burst pressure and compliance. LC and HC grafts had burst pressure of 691.6 ± 104.2 mmHg and 439.2 ± 72.0 mmHg, respectively (Fig. 2B). The compliance of LC and HC grafts is $1.23 \pm 0.16\%/40$ mmHg and $1.83 \pm 0.27\%/40$ mmHg, respectively, representing 48% and 71% matching to the compliance of native rabbit carotid artery ($2.57 \pm 0.27\%/40$ mmHg) (Fig. 2C). The results demonstrated that by using dip casting fabrication, we were able to fabricate PVA grafts with significantly different compliance without the need to alter material chemistry. The HC grafts also maintained sufficient burst pressure.

3.2. *In vivo* performance of grafts with low compliance (LC) and high compliance (HC) in end-to-side model

In order to study the effect of compliance on graft performance in an end-to-side anastomosis model, we implanted 5 LC grafts and 4 HC grafts in rabbit right common carotid artery, as shown in Fig. 3A. The grafts had inner diameter of 1.7 mm
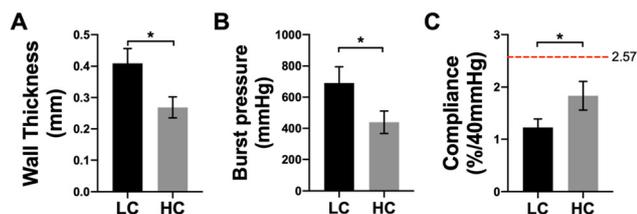
Fig. 2 Mechanical properties of low compliance (LC) grafts and high compliance (HC) grafts. (A) Wall thickness, (B) burst pressure, and (C) compliance of LC and HC grafts. $n = 3$, * indicates a significant difference using *t*-test with $p < 0.05$. Red dash line indicates the compliance of native rabbit carotid artery.
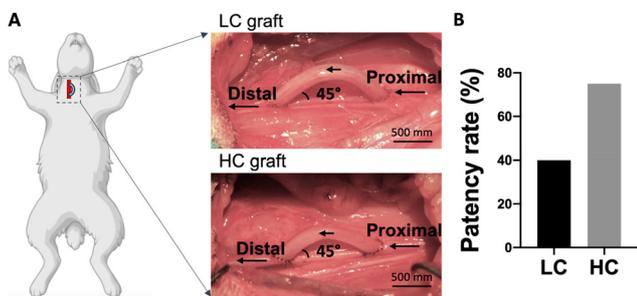
Fig. 3 Implantation of PVA small diameter vascular grafts with low compliance (LC) and high compliance (HC) in rabbit right common carotid artery in an end-to-side anastomotic model. (A) Representative photos of low compliance (LC) PVA grafts and high compliance (HC) PVA grafts after implantation. (B) 1-month patency rate of LC and HC grafts.

and length of 2 cm. A curvature was created during the graft fabrication to prevent kinking. Additionally, the implantation angle at the two anastomoses was approximately 45°, and the distance between the 2 anastomoses was around 1.5 cm. After 1 month implantation, we found 2 out of 5 LC grafts were patent (40% patency), while 3 out of 4 HC grafts were patent (75% patency) (Fig. 3B).

We used ultrasound imaging to detect the blood flow inside the implanted grafts at both midpoint (day 10–14) and endpoint (day 27–30). We detected stronger blood flow inside the HC grafts compared to LC grafts at both midpoint and endpoint (Fig. 4A). Doppler measurement of blood flow velocity showed that flow velocity in HC grafts was higher at both midpoint and endpoint, and at the endpoint, the flow velocity in HC grafts was significantly higher than in LC grafts (Fig. 4B).

3.3. Histological analysis of explanted low compliance (LC) and high compliance (HC) grafts

Anastomotic intimal hyperplasia formation has been identified as the main cause of failure of small diameter vascular grafts.[31] H&E staining was done at the proximal and distal anastomoses for both LC and HC grafts to analyze the intimal hyperplasia formation (Fig. 5A and B). HC grafts showed decreased area of intimal hyperplasia compared to LC grafts at both proximal and distal anastomoses. Additionally, intimal hyperplasia was formed mainly on the arteries. No intimal hyperplasia was observed on the graft luminal surfaces regardless of graft compliance. Quantification results showed that the intimal hyperplasia on HC grafts was significantly lower than that on LC grafts at the proximal anastomosis, while slightly but not significantly lower at the distal anastomosis. A noticeable animal-to-animal variation of intimal hyperplasia area was observed at the distal anastomosis of HC grafts (Fig. 5B).

Masson's trichrome staining demonstrated the presence of collagen and muscle fibers in the intimal hyperplasia (Fig. 6A). Quantification results showed that, when dividing the area of collagen and muscle fibers by the total luminal area, the percentage of collagen and the percentage of muscle fibers for LC grafts at both the proximal and distal anastomoses were higher compared to those for HC grafts, although the differences were not statistically significant (Fig. 6B). We further divided the area of collagen and the area of muscle fibers by the total area of intimal hyperplasia, no significant difference was observed.

Immunohistochemistry staining of α-smooth muscle actin (α-SMA) showed abundant vascular smooth muscle cells in the intimal hyperplasia region of both LC grafts and HC grafts (Fig. 7). More α-SMA positive area was observed in the intimal hyperplasia of HC grafts. The quantification of α-SMA positive area is as shown in Fig. 10A. HC grafts had slightly higher percentage of α-SMA positive region in proximal anastomoses and significantly higher α-SMA positive region in the distal anastomoses compared to LC grafts. Smooth muscle myosin heavy chain (SM MHC) is a specific marker of differentiated smooth muscle cells.[32] The immunohistochemistry staining for SM
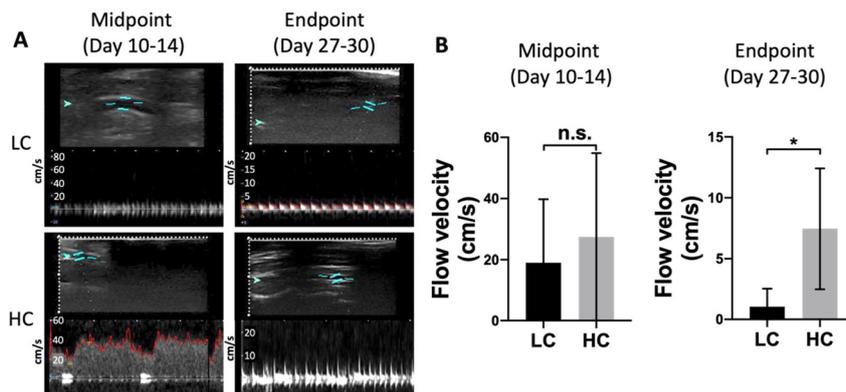
Fig. 4 *In vivo* patency of PVA small diameter vascular grafts with low compliance (LC) and high compliance (HC). (A) Representative ultrasound images of blood flow inside the grafts at midpoint (day 10−14) and endpoint (day 27−30). Red arrow indicates the direction of bloof flow. (B) Midpoint and endpoint flow velocity measurement. *n* = 5 for LC grafts, and *n* = 4 for HC grafts. * indicates a significant difference using *t*-test with *p* < 0.05.
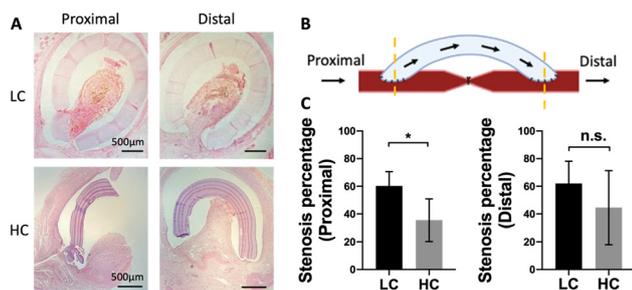

Fig. 5 Intimal hyperplasia formation at the anastomoses of grafts with low compliance (LC) and high compliance (HC). (A) Representative hematoxylin and eosin (H&E) staining images of proximal and distal anastomoses. Part of the PVA graft were broken during the tissue processing and staining procedure in the HC graft. (B) Schematic diagram of locations of proximal and distal anastomoses. (C) Intimal hyperplasia percentage at proximal and distal anastomoses. *n* = 5 for LC grafts, and *n* = 4 for HC grafts. * indicates a significant difference using *t*-test with *p* < 0.05. N.S. indicates no significant difference.

MHC of LC and HC grafts at the anastomoses region is as shown in Fig. 8. Higher percentage of MHC positive region was observed in the proximal anastomoses of LC grafts and both proximal and distal anastomoses of HC grafts. The quantification results showed that the MHC positive region at the distal anastomoses of HC grafts was significantly higher than that of LC grafts (Fig. 10B). Smooth muscle 22-α (SM22α) has been shown to modulate SMC phenotype.[33] We stained the anastomoses with SM22α (Fig. 9) and quantified the percentage of positive region. Both the LC and HC grafts havd high percentage of SM22α positive area at proximal and distal anastomoses (Fig. 10C).

3.4. *In vivo* performance of low compliance (LC) and high compliance (HC) grafts in end-to-end model

In our previous study, we had implanted straight compliance matching PVA small diameter vascular grafts with 1 mm

internal diameter in rabbit left femoral artery using an end-to-end anastomosis technique.[34,35] In addition to the compliance matching grafts, we also implanted grafts with lower compliance to study the effect of compliance on graft performance and patency in an end-to-end model. Two groups of PVA groups were implanted (ESI Fig. 1†). Compliance mismatch PVA graft group had average compliance of 4.917%/40mmHg, while the compliance matching group had average compliance of 6.491%/40mmHg, which is comparable to the compliance of rabbit femoral artery (5.9 ± 0.5%/40 mmHg).[34] The angiography showed that the 2 grafts in compliance matching group were both patent, while the 2 grafts in the compliance mismatch group were occluded (ESI Fig. 2†). The results suggested that the compliance matching between artificial graft and native artery could potentially improve graft patency.

4. Discussion

The patency of synthetic small diameter vascular grafts remains disappointing due to fast occlusion. Intimal hyperplasia formation at the anastomosis region has been identified as one of the main causes of failure.[36] Vascular grafts made of synthetic materials typically have a significantly lower compliance than native arteries, which causes localized flow disturbance, adverse shear stress, and altered suture-line stress,[15,37] thus leading to the dysfunction of endothelial cells, activation of smooth muscle cells, and consequently intimal hyperplasia formation. Previous *in vivo* studies showed that graft patency can be improved by matching the compliance of synthetic graft and the artery; however, most were comparing synthetic vascular grafts with autografts or comparing synthetic grafts made of different materials. Thus, a synthetic material that can modulate graft compliance without affecting material chemistry or topography is needed to understand the effect of compliance on intimal hyperplasia formation and graft patency. Our previous studies demonstrated that STMP-cross-
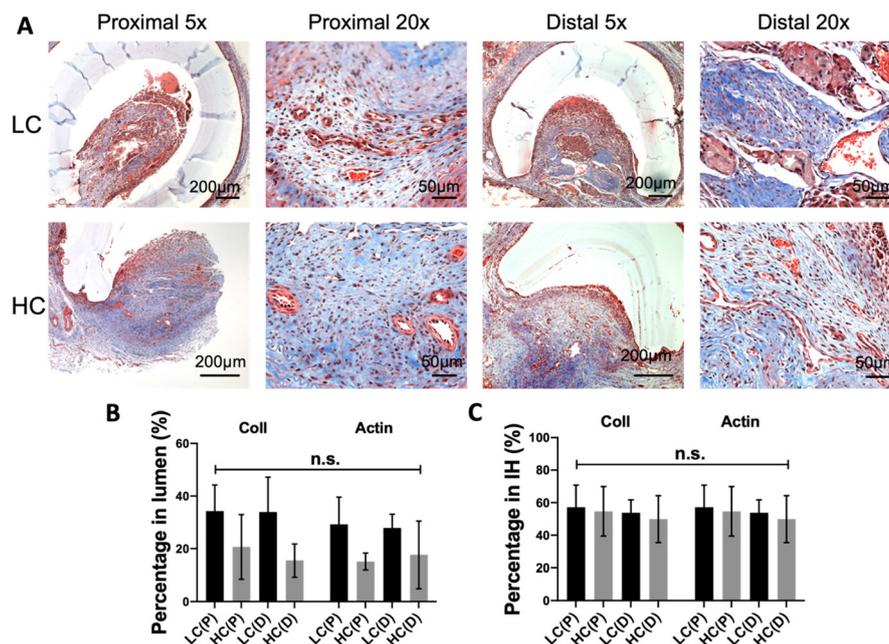
Fig. 6 Composition of intimal hyperplasia formed at the anastomoses of grafts with different compliance. (A) Representative Masson's trichrome staining images of the stenosis in proximal and distal anastomose. (B) Percentage of collagen and muscle fiber area in the lumen of the grafts. (C) Percentage of collagen and muscle fiber area in the stenosis. $n = 5$ for LC grafts, and $n = 4$ for HC grafts. N.S. indicates no significant difference.
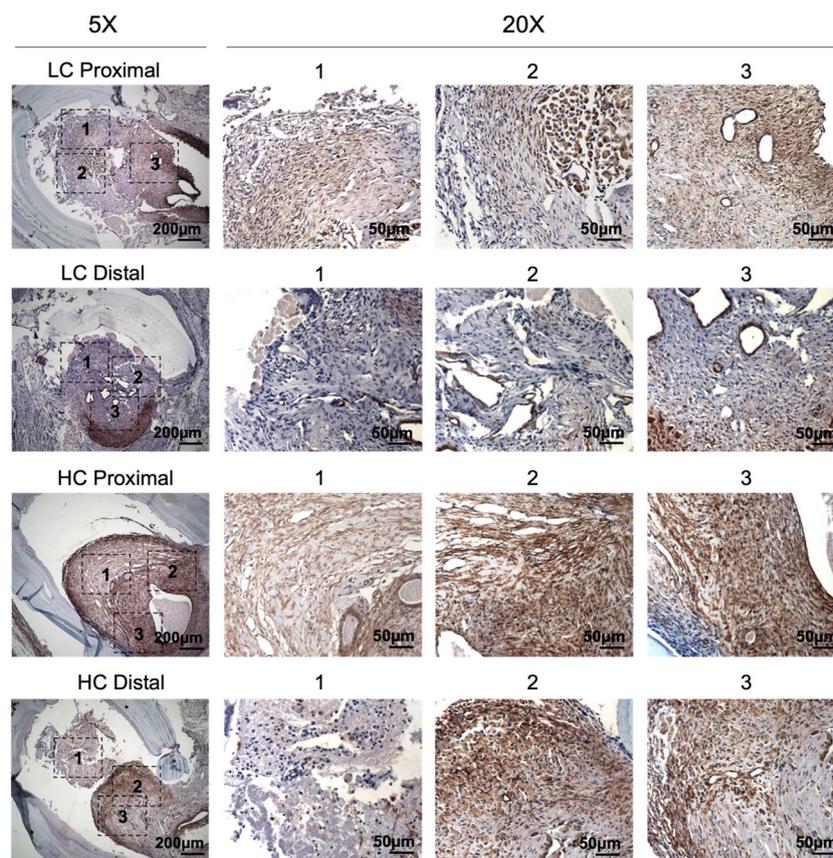

Fig. 7 Immunohistochemistry staining of α-smooth muscle actin (α-SMA) for the PVA low compliance (LC) grafts and high compliance (HC) grafts at the proximal and distal anastomoses.
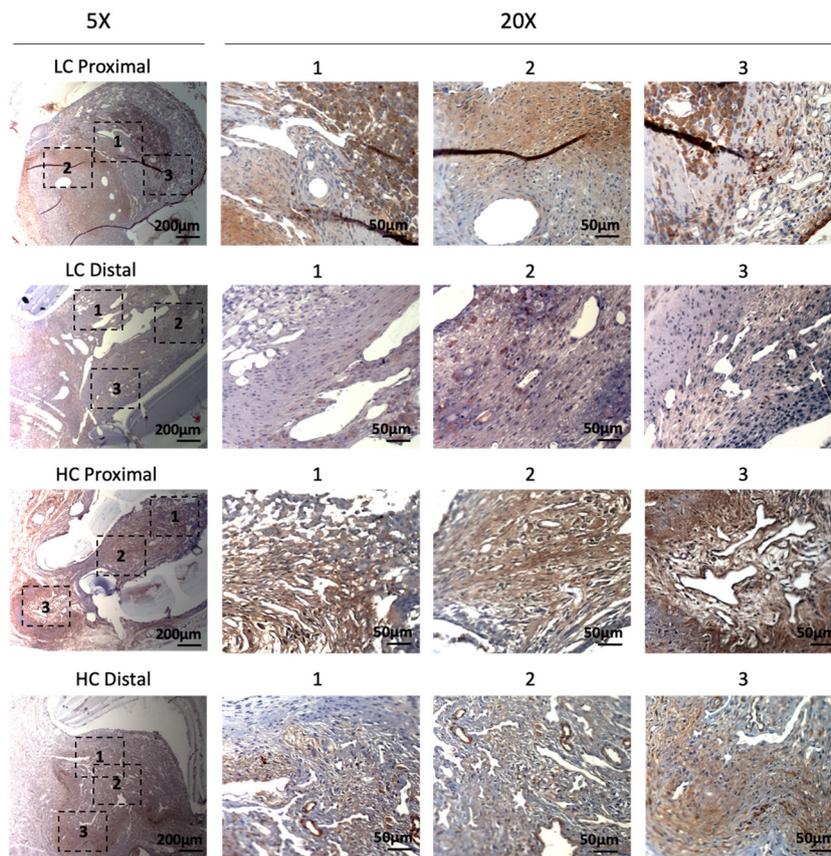
Fig. 8 Immunohistochemistry staining of smooth muscle myosin heavy chain (SM MHC) for the PVA low compliance (LC) grafts and high compliance (HC) grafts at the proximal and distal anastomoses.

linked PVA is a promising vascular graft material and dip casting method can be used to fabricate PVA tubular grafts.[26,35] We found that the mechanical properties of fabricated PVA tubular grafts could be modulated by manipulating the fabrication parameters.[28] In this study, we were able to fabricate PVA small diameter vascular grafts with different compliance by changing the number of dipping layers without the need of altering material chemistry. The HC grafts fabricated with 6 layers of dip coating had significantly lower wall thickness and significantly higher compliance compared to LC grafts, which were fabricated with 8 layers of dip coating. More importantly, although the wall thickness of HC grafts was significantly decreased, both HC and LC grafts still maintained sufficient burst pressure to withstand physiological blood pressure, thus allowing us to study the relevance between graft compliance and patency *in vivo*. We previously demonstrated that gamma irradiation is a suitable sterilization method for PVA grafts.[29] In the previous study, we compared the mechanical properties of PVA grafts before and after gamma irradiation. The gamma irradiation did not alter the swelling, Young's modulus, burst pressure, and suture retention of the PVA grafts. The compliance of both thick and thin PVA grafts was increased by gamma irradiation, but grafts with thicker wall still had significantly lower compliance than grafts with

thinner wall. Thus, we sterilized the HC and LC grafts with gamma-irradiation prior to implantation in this study.

To study the effect of compliance on intimal hyperplasia formation and graft patency, we implanted both the HC and LC grafts in a rabbit right common carotid artery end-to-side anastomosis model, where a graft needed to be bended to connect the 2 ends of the graft to the artery wall. Graft kinking has been a concern when using a straight graft to replace curved arterial arch, which causes blood flow turbulence and increased thrombus formation.[38] In our previous study, when using straight ePTFE graft in end-to-side anastomosis model, a kink was formed on the graft; while with PVA grafts that were pre-curved, the grafts were easily attached to the arterial wall without causing significant kinking.[39] Thus, in this study, both HC and LC grafts were fabricated into curved shape to prevent kinking. In end-to-side anastomosis model, the anastomotic junction angle affects the shear stress and flow patterns.[40–42] An anastomotic junction angle of 45° has been shown to induce low flow separation and high shear stress around the anastomosis zones, thus producing low amount of intimal thickening.[40] Hence, in our study, we cut the two ends of the graft prior to implantation and implanted the grafts with an junction angle of 45°. Previous simulation studies using computational modeling reported that a greater compli-
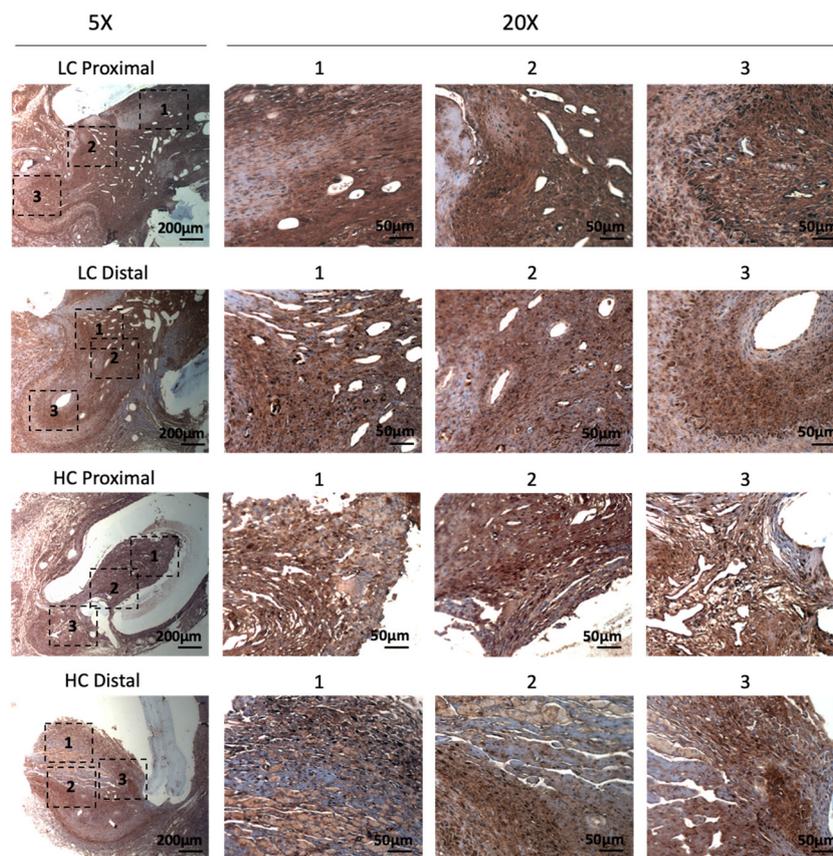
Fig. 9 Immunohistochemistry staining of smooth muscle protein 22-α (SM22α) for the PVA low compliance (LC) grafts and high compliance (HC) grafts at the proximal and distal anastomoses.
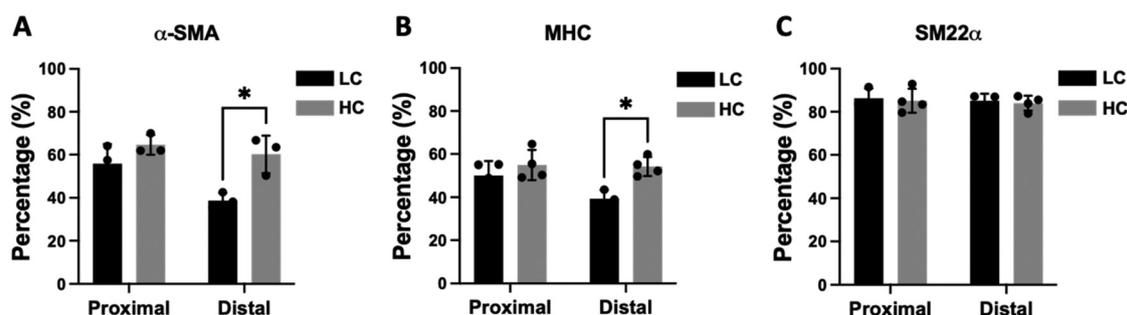

Fig. 10 Quantification of α-smooth muscle actin (α-SMA) (A), myosin heavy chain (MHC) (B), and smooth muscle protein 22-α (SM22α) (C) positive area. $n = 5$ for LC grafts and $n = 4$ for HC grafts. * indicates a significant difference of $p < 0.05$ using two-way ANOVA with Sidak's *post hoc* test.

ance mismatch between the synthetic graft and native artery has more adverse effect on blood flow profile, causing more severe flow separation and decreased wall shear stresses.[22,43] This phenomenon has been hypothesized to initiate and amplify the intimal hyperplasia formation. However, these results were yet to be verified *in vivo*. In this study, we used a rabbit right common carotid artery end-to-side anastomosis model to study the effect of compliance on graft patency *in vivo*. Although the compliance of HC grafts is still lower than native rabbit carotid artery (2.57%/40 mmHg), HC grafts

showed a higher 1-month patency rate, stronger blood flow and reduce intimal hyperplasia area compared to LC grafts (Fig. 3–5). The results are in line with computational modeling and demonstrated that the decrease in compliance discrepancy between a synthetic graft and artery could increase the patency rate and reduce intimal hyperplasia formation. In end-to-side anastomosis model, spatial distribution of intimal hyperplasia was reported to be preferentially located around the heel and toe at the anastomotic junctions and floor of the native arteries, due to the flow separation and decreased wall

shear stress around those regions.[44,45] In our studies, we also observed that the intimal hyperplasia was mainly formed at the floor of native arteries. Although many studies focused on distal anastomotic intimal hyperplasia,[22,46] intimal hyperplasia has also been reported to be formed around proximal anastomoses.[47] We observed comparable amount of intimal hyperplasia at both proximal and distal anastomoses. We speculate that the hemodynamics changed due to both graft compliance mismatch and anastomotic geometry and the surgical trauma cause activation of endothelial cells and smooth muscle cells in the current end-to-side anastomosis model, which together lead to intimal hyperplasia formation. Additionally, the PVA grafts we used had higher wall thickness compared to the native artery, which has been shown to present higher risk of surgical trauma, thus further amplifying the formation of intimal hyperplasia.[43,48] Using the same animal model, we previously implanted ePTFE small diameter vascular grafts. The compliance of the ePTFE vascular grafts was around 0.704%/40 mmHg.[39] 2 out 3 ePTFE grafts were patent. In patent ePTFE grafts, intimal hyperplasia was only observed on the surface of ePTFE grafts, while in occluded ePTFE graft, significant amount of intimal hyperplasia was observed both in floor of the artery and on the surface of ePTFE grafts at both anastomoses.[39] Interestingly, different from ePTFE grafts and other synthetic vascular grafts, no intimal hyperplasia was formed on the surface of PVA grafts. We speculate that this phenomenon could potentially be due to the hydrophilicity and bioinert nature of PVA hydrogels.

Intimal hyperplasia formation is characterized by vascular smooth muscle cell migration, proliferation, and secretion of extracellular matrix.[49] Many studies have suggested that compliance mismatch at the anastomoses leads to increased vascular smooth muscle cell proliferation and migration, and induces phenotype changes of smooth muscle cells from contractile to proliferative phenotype.[22] We did histological staining and analysis to study the composition of intimal hyperplasia. In our Masson's trichrome staining, the presence of collagen and smooth fibers were demonstrated, and the percentage of collagen and the percentage of fiber area in the lumen of the LC grafts were slightly but not significantly higher than that of HC grafts at both proximal and distal anastomoses. However, the composition percentages of collagen and of fiber in the intimal hyperplasia were comparable between LC and HC grafts. Additionally, immunohistochemistry staining of α-SMA showed abundant α-SMA + cells in both LC and HC grafts, indicating the presence of smooth muscle cells (Fig. 6 and 7). We observed stronger α-SMA expression in the anastomotic IHC section of most HC grafts compared to LC grafts. α-SMA is a marker of contractile smooth muscle cells,[50,51] and α-SMA has been reported to negatively regulate the smooth muscle cell migration and proliferation.[52] Loss of α-SMA has also been shown to contribute to increased SMC hyperplasia *in vivo*.[53,54] We speculate that in our study, the higher compliance synthetic vascular grafts might have induced stronger α-SMA expression compared to lower compliance grafts, thus reducing intimal hyperplasia formation. The staining of smooth muscle contractile protein, MHC, further supported our speculation. We found that HC grafts had more MHC positive region especially at the distal anastomoses compared to LC grafts, suggesting that more contractile cells were present in the HC grafts than LC grafts at the distal anastomoses.

Many computational simulation studies have reported that compliance affects intimal hyperplasia formation not only in end-to-side anastomosis model but also in end-to-end anastomosis model.[14,22,55] Our previous studies implanted straight PVA small diameter vascular grafts with inner diameter of approximately 1 mm in rabbit left femoral artery end-to-end anastomosis model.[34,35] As a preliminary study when we compared the 1 mm PVA vascular graft with lower compliance, we showed that compliance matching grafts were patent after 14 days of implantation, while the mismatch groups were occluded. This suggests that in end-to-end anastomosis, reducing compliance mismatch is also promising in improving vascular graft patency.

5. Conclusion

In summary, in this study we successfully fabricated PVA-based small diameter vascular grafts with different mechanical properties and studied the role of compliance in graft patency and intimal hyperplasia formation *in vivo*. We demonstrated that compliance mismatch between the graft and artery had a direct effect on the intimal hyperplasia formation and graft patency. Additionally, our proof-of-concept *in vivo* study showed the grafts with higher compliance could potentially improve graft patency, increase smooth muscle cell contractility, and reduced intimal hyperplasia formation.

Conflicts of interest

There are no conflicts to declare.

Acknowledgements

help with the rabbit study, and Dr Adrian Chee, Dr Billy Yat Shun Yiu, and Dr Marek Kukumberg for taking the ultrasound measurements in the *in vivo* work.

References

1 W. H. Organization, Cardiovascular diseases (CVDs), https://www.who.int/en/news-room/fact-sheets/detail/cardiovascular-diseases-(cvds), (accessed June 11, 2021).
2 X. Wang, P. Lin, Q. Yao and C. Chen, *World J. Surg.*, 2007, **31**, 682–689.
3 Y. Roina, F. Auber, D. Hocquet and G. Herlem, *Mater. Today Chem.*, 2021, **20**, 100412.
4 S. Pashneh-Tala, S. MacNeil and F. Claeyssens, *Tissue Eng., Part B*, 2015, **22**, 68–100.
5 B. H. Walpoth and G. L. Bowlin, *Expert Rev. Med. Devices*, 2005, **2**, 647–651.
6 Y. Jeong, Y. Yao and E. K. F. Yim, *Biomater. Sci.*, 2020, **8**, 4383–4395.
7 Y. Zhuang, C. Zhang, M. Cheng, J. Huang, Q. Liu, G. Yuan, K. Lin and H. Yu, *Bioact. Mater.*, 2021, **6**, 1791–1809.
8 R. N. Baird, I. G. Kidson, G. J. L'Italien and W. M. Abbott, *Am. J. Physiol.: Heart Circ. Physiol.*, 1977, **233**, H568–H572.
9 R. Baird and W. Abbott, *Lancet*, 1976, **308**, 948–950.
10 L. Li, C. M. Terry, Y.-T. E. Shiu and A. K. Cheung, *Kidney Int.*, 2008, **74**, 1247–1261.
11 H. Haruguchi and S. Teraoka, *J. Artif. Organs*, 2003, **6**, 227–235.
12 A. Remuzzi and B. Ene-Iordache, *Clin. J. Am. Soc. Nephrol.*, 2013, **8**, 2186.
13 A. Acuna, A. G. Berman, F. W. Damen, B. A. Meyers, A. R. Adelsperger, K. C. Bayer, M. C. Brindise, B. Bungart, A. M. Kiel, R. A. Morrison, J. C. Muskat, K. M. Wasilczuk, Y. Wen, J. Zhang, P. Zito and C. J. Goergen, *J. Biomech. Eng.*, 2018, **140**, 080801.
14 A. A. Owida, H. Do and Y. S. Morsi, *Comput. Methods Programs Biomed.*, 2012, **108**, 689–705.
15 P. D. Ballyk, C. Walsh, J. Butany and M. Ojha, *J. Biomech.*, 1997, **31**, 229–237.
16 V. S. Sottiurai, S. L. Sue, E. L. Feinberg II, W. L. Bringaze, A. T. Tran and R. C. Batson, *Eur. J. Vasc. Surg.*, 1988, **2**, 245–256.
17 V. S. Sottiurai, J. S. T. Yao, R. C. Batson, S. L. Sue, R. Jones and Y. A. Nakamura, *Ann. Vasc. Surg.*, 1989, **3**, 26–33.
18 L. J. Brossollet, *Int. J. Artif. Organs.*, 1992, **15**, 579–584.
19 W. M. Abbott, J. Megerman, J. E. Hasson, G. L'Italien and D. F. Warnock, *J. Vasc. Surg.*, 1987, **5**, 376–382.
20 S. F. C. Stewart and D. J. Lyman, *Ann. Biomed. Eng.*, 2004, **32**, 991–1006.
21 M. H.-D. Wu, Q. Shi, L. R. Sauvage, S. Kaplan, N. Hayashida, M. D. Patel, A. R. Wechezak and M. W. Walker, *Ann. Vasc. Surg.*, 1993, **7**, 156–168.
22 A. Post, P. Diaz-Rodriguez, B. Balouch, S. Paulsen, S. Wu, J. Miller, M. Hahn and E. Cosgriff-Hernandez, *Acta Biomater.*, 2019, **89**, 84–94.
23 G. Paradossi, F. Cavalieri, E. Chiessi, C. Spagnoli and M. K. Cowman, *J. Mater. Sci.: Mater. Med.*, 2003, **14**, 687–691.
24 S. Jiang, S. Liu and W. Feng, *J. Mech. Behav. Biomed. Mater.*, 2011, **4**, 1228–1233.
25 M. F. Cutiongco, D. E. Anderson, M. T. Hinds and E. K. Yim, *Acta Biomater.*, 2015, **25**, 97–108.
26 M. Chaouat, C. Le Visage, W. E. Baille, B. Escoubet, F. Chaubet, M. A. Mateescu and D. Letourneur, *Adv. Funct. Mater.*, 2008, **18**, 2855–2861.
27 M. F. Cutiongco, S. H. Goh, R. Aid-Launais, C. Le Visage, H. Y. Low and E. K. F. Yim, *Biomaterials*, 2016, **84**, 184–195.
28 Y. Jeong, Y. Yao, T. H. Mekonnen and E. K. F. Yim, *Front. Mater.*, 2021, **7**, 595295.
29 G. Pohan, S. Mattiassi, Y. Yao, A. M. Zaw, D. E. J. Anderson, M. F. A. Cutiongco, M. T. Hinds and E. K. F. Yim, *Tissue Eng., Part A*, 2020, **26**, 1077–1090.
30 Y. Yao, Y. Jeong, A. M. Zaw, M. Kukumberg and E. K. F. Yim, in *Vascular Tissue Engineering: Methods and Protocols*, ed. F. Zhao and K. W. Leong, Springer US, New York, NY, 2022, pp. 177–189, DOI: 10.1007/978-1-0716-1708-3_15.
31 R. S. Keynton, M. M. Evancho, R. L. Sims, N. V. Rodway, A. Gobin and S. E. Rittgers, *J. Biomech. Eng.*, 2001, **123**, 464–473.
32 A. T. Nguyen, D. Gomez, R. D. Bell, J. H. Campbell, A. W. Clowes, G. Gabbiani, C. M. Giachelli, M. S. Parmacek, E. W. Raines, N. J. Rusch, M. Y. Speer, M. Sturek, J. Thyberg, D. A. Towler, M. C. Weiser-Evans, C. Yan, J. M. Miano and G. K. Owens, *Circ. Res.*, 2013, **112**, 17–22.
33 S. Feil, F. Hofmann and R. Feil, *Circ. Res.*, 2004, **94**, 863–865.
34 M. F. Cutiongco, M. Kukumberg, J. L. Peneyra, M. S. Yeo, J. Y. Yao, A. J. Rufaihah, C. Le Visage, J. P. Ho and E. K. Yim, *Front. Bioeng. Biotechnol.*, 2016, **4**, 44.
35 M. F. A. Cutiongco, R. K. T. Choo, N. J. X. Shen, B. M. X. Chua, E. Sju, A. W. L. Choo, C. Le Visage and E. K. F. Yim, *Front. Bioeng. Biotechnol.*, 2015, **3**, 3.
36 F. O. Obiweluozor, G. A. Emechebe, D.-W. Kim, H.-J. Cho, C. H. Park, C. S. Kim and I. S. Jeong, *Cardiovasc. Eng. Technol.*, 2020, **11**, 495–521.
37 T. Frauenfelder, E. Boutsianis, T. Schertler, L. Husmann, S. Leschka, D. Poulikakos, B. Marincek and H. Alkadhi, *Biomed. Eng. Online*, 2007, **6**, 35–35.
38 M. Misfeld, M. Scharfschwerdt and H.-H. Sievers, *Ann. Thorac. Surg.*, 2004, **78**, 1060–1063.
39 Y. Yao, A. M. Zaw, D. E. J. Anderson, M. T. Hinds and E. K. F. Yim, *Biomaterials*, 2020, **249**, 120011.
40 R. S. Keynton, S. E. Rittgers and M. C. S. Shu, *J. Biomech. Eng.*, 1991, **113**, 458–463.
41 Z. S. Jackson, H. Ishibashi, A. I. Gotlieb and B. L. Langille, *J. Vasc. Surg.*, 2001, **34**, 300–307.
42 J. T. Kim, H. Kim and H. S. Ryou, *Appl. Sci.*, 2021, **11**, 8160.
43 M. Bouchet, M. Gauthier, M. Maire, A. Ajji and S. Lerouge, *Mater. Sci. Eng., C*, 2019, **100**, 715–723.

44 F. Migliavacca and G. Dubini, *Biomech. Model. Mechanobiol.*, 2005, **3**, 235–250.

45 H. S. Bassiouny, S. White, S. Glagov, E. Choi, D. P. Giddens and C. K. Zarins, *J. Vasc. Surg.*, 1992, **15**, 708–717.

46 W. Trubel, A. Moritz, H. Schima, F. Raderer, R. Scherer, R. Ullrich, U. Losert and P. Polterauer, *ASAIO J.*, 1994, **40**, M273–M278.

47 I. Baek, J. Hwang, J. Park, H. Kim, J.-S. Park and D. J. Kim, *J. Vasc. Surg.*, 2015, **61**, 1575–1582.

48 K. J. Furdella, S. Higuchi, A. Behrangzade, K. Kim, W. R. Wagner and J. P. Vande Geest, *Acta Biomater.*, 2021, **123**, 298–311.

49 M. S. Lemson, J. H. M. Tordoir, M. J. A. P. Daemen and P. J. E. H. M. Kitslaar, *Eur. J. Vasc. Endovasc. Surg.*, 2000, **19**, 336–350.

50 S. S. M. Rensen, P. A. F. M. Doevendans and G. J. J. M. van Eys, *Neth. Heart J.*, 2007, **15**, 100–108.

51 S.-A. Xie, T. Zhang, J. Wang, F. Zhao, Y.-P. Zhang, W.-J. Yao, S. S. Hur, Y.-T. Yeh, W. Pang, L.-S. Zheng, Y.-B. Fan, W. Kong, X. Wang, J.-J. Chiu and J. Zhou, *Biomaterials*, 2018, **155**, 203–216.

52 L. Chen, A. DeWispelaere, F. Dastvan, W. R. A. Osborne, C. Blechner, S. Windhorst and G. Daum, *PLoS One*, 2016, **11**, e0155726.

53 C. L. Papke, J. Cao, C. S. Kwartler, C. Villamizar, K. L. Byanova, S.-M. Lim, H. Sreenivasappa, G. Fischer, J. Pham, M. Rees, M. Wang, C. Chaponnier, G. Gabbiani, A. Y. Khakoo, J. Chandra, A. Trache, W. Zimmer and D. M. Milewicz, *Hum. Mol. Genet.*, 2013, **22**, 3123–3137.

54 Y.-n. Zhang, B.-d. Xie, L. Sun, W. Chen, S.-L. Jiang, W. Liu, F. Bian, H. Tian and R.-K. Li, *J. Cell. Mol. Med.*, 2016, **20**, 1049–1061.

55 S. F. C. Stewart and D. J. Lyman, *Ann. Biomed. Eng.*, 2004, **32**, 991–1006.